Tellus (2006), 58A, 404–415
Printed in Singapore. All rights reserved

Copyright © Blackwell Munksgaard, 2006
TELLUS

Meridional thermal field of a coupled ocean-atmosphere system: a conceptual model

By HSIEN-WANG OU*, *Division of Ocean and Climate Physics, Lamont-Doherty Earth Observatory of Columbia University, 61 Route 9W, Palisades, NY 10964, USA*

(Manuscript received 23 May 2005; in final form 1 November 2005)

ABSTRACT

This paper constitutes the author's continuing effort in the construction of a minimal theory of the earth's climate. In an earlier paper published in the Journal of Climate in 2001, this author has derived the global-mean fields of an aquatic planet forced by the solar insolation, which provide the necessary constraints for the present derivation of the meridional thermal field. The model closure invokes maximized entropy production (MEP), a thermodynamic principle widely used in turbulence and climate studies.

Based on differing convective regimes of the ocean and atmosphere, both fluids are first reduced two thermal masses with aligned fronts, consistent with a minimal description of the observed field. Subjected to natural bounds, a robust solution is then found, characterized by an ice-free ocean, near-freezing cold fluid masses, mid-latitude fronts, and comparable ocean and atmosphere heat transports. The presence of polar continents, however, sharply reduces the ocean heat transport outside the tropics, but leaves the thermal field largely unchanged.

Given the limitation of an extremely crude model, the deduced thermal field nonetheless seems sensible, suggesting that the model has captured the physics for a minimal account of the observed field. Together with the above-mentioned paper, the model reinforces the pre-eminent role of the triple point of water in stabilizing the surface temperature – against changing external condition. Such internal control is made possible by the turbulent nature of the climate fluids, which necessitates a selection rule based on extremization.

1. Introduction

What endows the earth's climate with its essential character is a question that has long intrigued climate theorists. Although we know reasonably well the inner working of the ocean and atmosphere in isolation, this understanding does not necessarily translate to the climate as a whole, which is a manifest in toto of a single ocean-atmosphere system. A simple test of the understanding would be the derivation of the basic climate from first principles – free of empirical constraints, a quest not yet fulfilled.

One of course recognizes the complexity of the earth's climate system with its many interwoven pieces and practically infinite degrees of freedom, so any climate theory necessarily represents an extreme reductionist approach to the problem. But given that even the basic closure of the system remains uncertain, we shall go one step farther and seek a *minimal* model that is capable of producing a "sensible" climate. It should be stressed that this approach is diametrically opposite to that of the general circulation models, which strives for realism by incorporating *maximum* physics. But by forgoing complications associated with more realistic models, we hope to isolate and – hence – aid the understanding of the fundamental working of the system.

As a first step in our construction of a minimal theory of the climate, we have considered a one-dimensional (vertical) model to deduce the global-mean fields (Ou, 2001, hereafter Ou01). Although the solar constant constitutes the only external forcing, the surface temperature turns out to be narrowly bounded by intrinsic water properties – hence not particularly sensitive to the solar constant, which may possibly resolve the "young faint sun" paradox. Moreover, of some relevance to the present derivation, the surface temperature lies only slightly above the triple point of water (the difference being an order of magnitude smaller than its absolute temperature), in consistency with the observed climate. With the global-mean fields providing the necessary constraints, we seek now to derive the meridional thermal field when subjected to differential solar heating, the content of the present paper.

As in Ou01, the model closure invokes maximum entropy production (MEP), which has been applied to non-equilibrium thermodynamic systems of high degrees of freedom, and readers are referred to Ozawa et al. (2003) for a comprehensive review of the subject. The earth's climate system contains in effect infinite degrees of freedom, due in large part to the inherently turbulent

*Corresponding author.
e-mail: dou@ldeo.columbia.edu
DOI: 10.1111/j.1600-0870.2006.00174.x

nature of its fluids. On an intuitive level, such turbulence breaks the linkage between thermodynamic force and flux to render the macroscopic state indeterminant, which thus can be selected only by the extremum of some thermodynamic properties; and for a non-isolated system that exchanges energy with the surrounding, it turns out that the most probable selection rule is the maximization of the entropy production rate.

This principle of MEP was first applied to the climate problem by Paltridge's (1975). But despite the early success, its use has generated considerable debate for lack of physical justification. It was framed explicitly as a selection rule for turbulent fluids only a few years later (Sawada, 1981), a proper perspective unfortunately not widely noted. These factors have contributed to early criticisms of MEP, which – with the benefit of hindsight – are no longer valid. For example, some criticisms (e.g. Rodgers (1976)) are really directed at Prigogine's (1967) minimum entropy production principle, which depicts the evolution path of a linear system (as such, it imposes no additional constraint, see Jaynes (1980)) and hence bears no relation to MEP that selects among possible states. Then, there are questions about the "radiation" entropy flux (Essex, 1984), which again is a moot point since turbulence is internal to the fluid, so it is the "material" entropy production that should be maximized (Dewar, 2003; Ozawa et al., 2003).

Besides alleviating earlier concerns, recent advances on multiple fronts have significantly strengthened MEP as a viable counterpart to the second law for a nonlinear non-equilibrium thermodynamic system. On theoretical grounds, MEP can subsume the maximum energy conversion of Lorenz (1960) (see Ozawa et al., 2003), and is made equivalent to the maximum dissipation by Ziegler (1983). It unifies optimum (or upper-bound) theories of thermal convection and shear-induced turbulence (Malkus, 1954, 1956) (see Ozawa et al., 2001), and provides a statistical interpretation of Jaynes' (1957) information theory (Dewar, 2003). Computationally, MEP states have emerged from numerical simulations of thermal convection (Suzuki and Sawada, 1983; Minobe et al., 2000) and the GCM calculations of the atmosphere (Kleidon et al., 2003) and ocean (Shimokawa and Ozawa, 2002). In climate applications, MEP has been used to explain the lapse rate (Ozawa and Ohmura, 1997) and the mean temperature (Ou01) of the earth, and the temperature range of other planetary atmospheres (Lorenz et al., 2001). Beyond the climate, MEP has found empirical supports in crystal growth (Hill, 1990), and it has allowed a quantitative formulation of the Gaia hypothesis (Kleidon, 2004). With these developments, we are well justified to posit MEP as a working hypothesis in the construction of a climate theory.

The paper is organized as follows: in Section 2, we describe the model system and its reduction to thermal masses. In Section 3, we discuss the implementation of the MEP in terms of boundary entropy flux and a simplified differential heating scheme. In Section 4, we present the MEP solutions with incremental physics, which are then synthesized for its robust nature. The paper is concluded in Section 5 by additional discussion.

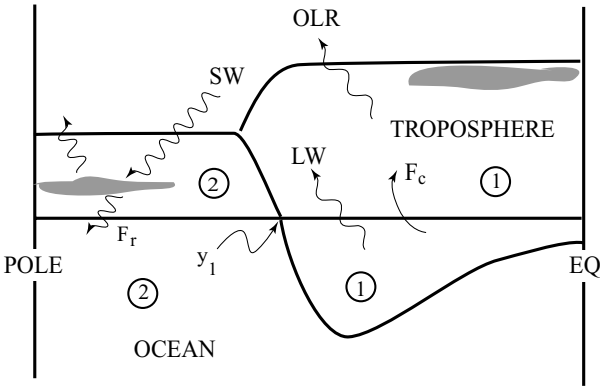

Fig. 1. A schematic model system consisting of a troposphere overlying a global ocean (only the hemispheric half is shown on account of symmetry). The incoming SW flux is partly reflected by clouds and the rest (F_r) absorbed by the ocean. The ocean heats the atmosphere by net LW flux and convective flux of sensible and latent heat (F_c). The heat is lost from the atmosphere via OLR, which completes the cycle. There are low and high clouds of distinct radiative properties, which are expelled to high and low latitudes, respectively. Both ocean and atmosphere are reduced to warm and cold masses (designated by numerals 1 and 2, respectively), with their boundaries aligned at the ocean surface.

2. Model system

We consider a minimal system of a troposphere overlying a global ocean (Fig. 1, only the hemispheric half is shown because of symmetry), although the effect of a small polar continent will be examined. The system is forced by differential solar heating, and the aim is to derive the meridional thermal field, taking as given relevant global-mean variables. In terms of the energy cycle, the incoming SW flux is partly reflected by the low clouds and the rest (F_r) absorbed by the ocean. The ocean warms the atmosphere by the LW flux and convective flux of sensible and latent heat (F_c), and the heat is lost from the system by the outgoing LW radiation (OLR), which may be partially blocked by the high clouds. The latitudinal variation of above fluxes causes differential heating of the fluids, resulting in poleward heat transports in the ocean (F_o) and atmosphere (F_a), which are to be determined in conjunction with the temperature field.

As in Ou01, clouds are divided into low clouds at the lifting condensation level and high clouds at the tropopause. Both are assumed to have small thickness, so their top and bottom have about the same temperatures. Because of their different composition and water density, both cloud types are assumed opaque in the LW band, but only low clouds have strong SW albedo (Liou, 1992). These properties, while crude, are sufficient for the later deduction of the cloud tendency and its qualitative effect on the differential heating.

Since the ocean is insulated at the bottom (neglecting the geothermal heating), its surface contains both heating and cooling regions. Based on the laboratory experiment on such a differentially heated fluid (Rossby, 1965), we infer that the bulk of the fluid would be homogenized by "free" convection from the

cooled surface, which is separated from the heated surface by a conductive layer. In the real ocean, however, there is wind stirring at the surface, which would replace the conductive layer by a "forced" convective layer. In the vertical, the process is similar to the deepening of the mixed layer in one-dimensional models, but it is extended here to a two-dimensional thermal mass, which requires horizontal mixing as well. For this, one may invoke ubiquitous eddies populated in the warm layer where there is ample supply of the available potential energy.

In other words, the differing mixing regimes of forced and free convection provide a rationale for dividing the ocean into warm and cold masses, separated by a boundary that outcrops at the surface – an approximation consistent with a minimal description of the observed ocean. The two thermal masses correspond to the warm- and cold-water spheres (see Neumann and Pierson, 1966, their Fig. 14.37), their boundary – the permanent thermocline, and its surface outcrop – the subtropical front. It is indeed their observed prominence that led to the widely used two-layer approximation in ocean circulation theories (e.g. Veronis (1973)).

In contrast to the ocean, the troposphere is heated from below and cooled above by OLR, hence it is globally convective. But with the ocean surface reduced to two thermal bands, it is seen later (Section 4.1) that MEP implies the same for the surface air. With free convection, the troposphere is then reduced to two thermal masses as well, just like the ocean, except the thermal property that is conserved with air motion and hence homogenized is the equivalent potential temperature – as reflected in the observed moist-adiabatic lapse rate. The two air masses correspond to the tropical and polar air masses, and their boundary, the polar front – a description highly discernible in synoptic meridional sections (Palmen and Newton (1969), see Fig. 4.4). But because of the large north–south excursion of the front, the latter is heavily smoothed in zonal-mean sections.

To recap, based on differing convective regimes of the ocean and atmosphere, and the later application of MEP, they both are reduced to two thermal masses with aligned fronts, as sketched in Fig. 1. While this simplification limits its observational comparison to the broadest outline, it also facilitates a closure that is relatively free of empirical constraints, allowing in fact a more stringent test. As an aside, it should be mentioned that box models have been widely used in climate studies (Stommel, 1961; Marotzke and Stone, 1995), and the thermal masses deduced here allow these boxes be assigned physical entity and hence more directly interpreted.

3. Maximized entropy production

3.1. Boundary entropy flux

To see how MEP is to be applied, we begin with the local rate of change of entropy S (e.g. De Groot and Mazur, 1963)

$$\frac{dS}{dt} \equiv \frac{Q}{T} = -\frac{1}{T}\nabla \cdot \vec{F}, \tag{3.1}$$

where T is the temperature, Q, the heating rate, and $\vec{F}$, the heat flux. Integrating this equation over the fluid volume V and using the divergence theorem, one derives

$$\int_V \frac{dS}{dt} dV = \int_V \vec{F}\cdot\nabla\frac{1}{T} dV - \int_V \nabla\cdot\frac{\vec{F}}{T} dV$$
$$= -\int_V \frac{1}{T^2}\vec{F}\cdot\nabla T dV - \int_A \frac{1}{T}\vec{F}\cdot\hat{n} dA, \tag{3.2}$$

where A is the surface enclosing V and $\hat{n}$, its outward-normal unit vector. For a stationary state, one has then

$$\sigma \equiv -\int_V \frac{1}{T^2}\vec{F}\cdot\nabla T dV \tag{3.3}$$

$$= \int_A \frac{1}{T}\vec{F}\cdot\hat{n} dA, \tag{3.4}$$

or the entropy produced in the interior by irreversible processes (3.3) is exported through the boundary (3.4). With MEP maximizing the former, it maximizes the latter as well, which is easier to apply since one need not be concerned with myriad internal processes that may generate entropy (e.g. Pauluis and Held, 2002).

Since the internal entropy production is positive (the second law), the fluid is warmer where the heat enters than where it is lost; the maximization of this rate on account of MEP implies additionally that, for a given differential heating, the temperature contrast is maximized, opposite in fact that of an isolated system. As we shall see later, this tendency, when combined with the natural bound imposed by the freezing point of the water, strongly stabilizes the thermal field – perhaps the most significant finding of the theory.

Since MEP is posited as a selection rule for the turbulent fluid and since turbulence is internal to the fluid, these have obvious implications on its application. First, it should apply to the ocean and atmosphere *individually*,[1] which turns out to be a significant development since it obviates extraneous assumptions used by Paltridge (1975, 1978) and O'Brien and Stephens (1995) to close the problem. Second, the relevant boundary temperature for the radiative fluxes is the one when radiation interacts with the fluid, which could differ from the fluid temperature at the boundary. This incidentally discounts the relevance of the solar temperature in the application of MEP, a point of some contention (Essex, 1984), but clarified by Ozawa et al. (2001). Besides, it is plainly intuitive that a climatic state should sense only the solar insolation regardless its emitting temperature.[2] In any

[1] One may also invoke disparate timescales of the two fluids, so the atmosphere would adjust to MEP given any oceanic condition, which would adjust to MEP on a much longer timescale (Axel Kleidon, personal communication). This supposition in fact dovetails the model derivation.

[2] The solar emission temperature would affect the spectral composition of the solar radiation, which has greater effect on chemical and biological processes of the climate system (e.g. Kleidon, 2004).

event, (3.4) should be interpreted as a sum over different energy forms, if their boundary temperature differ, a subject discussed next.

For the ocean, since it emits and absorbs all radiation at its surface temperature, this is the only relevant boundary temperature, so no distinction needs to be made of radiative and convective fluxes in (3.4). For the atmosphere, the situation is naturally more complicated. For one thing, radiation can be absorbed or emitted by clouds, but, given their (assumed) thinness (Section 2), these processes occur at the same temperature and hence effectuate no net entropy flux through the fluid boundary. Since the SW flux and the LW flux in the spectral window do not otherwise interact with the atmosphere, we are left to consider only the LW flux in the absorption band. Across the lower boundary of the atmosphere, this flux is absorbed or emitted at near the surface air temperature (Swinbank, 1963), which thus may be taken as (approximately) the relevant boundary temperature (for all energy forms). Across the tropopause, the OLR in the absorption band is emitted at a constant temperature in the upper troposphere (being saturated by strong absorptivity of the water vapor, see Ou01), and if it is partly redirected downward by high clouds, the latter is re-absorbed at a similar temperature, which thus constitutes the upper boundary temperature for this flux.

Having identified the proper fluid temperature for radiative fluxes across the boundaries, we shall next consider the cloud distribution, which affects these fluxes and hence must be constrained internally for the closure of the problem.

3.2. Cloud distribution

Based on the radiative properties of clouds prescribed in Section 2, we shall deduce a spatial tendency for clouds based on MEP or, more specifically, by maximizing the differential heating in the ocean and atmosphere given any thermal field.

We first consider the low cloud, which is seen above to have little effect on the entropy flux out of the troposphere, and hence is not constrained by the atmospheric MEP. But the low cloud strongly cools the ocean as its blockage of the SW flux dominates its augmentation of the downward LW flux (limited to the spectral window), so to maximize the differential heating of the ocean would propel the low cloud to high latitudes. This deduction incidentally is consistent with Paltridge's (1975) solution of the (single) cloud cover, which corresponds to our low cloud given the radiative properties he used.

We next consider the high cloud, which has little effect on the ocean, since its SW albedo and its LW emission entering the ocean are both small (the latter due to the low emission temperature and its transmission only in the spectral window). But the high cloud does exert a strong heating of the atmosphere in the LW band, since it redirects part of the OLR downward to be reabsorbed by the atmosphere. To maximize the differential heating of the atmosphere thus would propel the high cloud to low latitudes – opposite the low cloud.

To recap, because of blockage of the SW flux into the ocean by low clouds and greenhouse warming of the atmosphere by high clouds, they are propelled by MEP to high and low latitudes, respectively. This sequestration of the two cloud types to the opposite ends of the hemisphere (as indicated in Fig. 1) – though based solely on thermodynamics and neglecting some well-known cloud-genesis processes – is nonetheless quite discernible from observations (see Fig. 3.21 of Hartmann (1994) and remember that the deduction is for an aquatic planet that contains no zonal asymmetry associated with land-sea contrast), a feature thus may possibly be explained. Given the (known) global covers for both cloud types (e.g. Ou01), the above tendency allows in principle the specification of the cloud distribution and hence its effect on the radiative fluxes, as discussed next.

3.3. Differential heating

We have plotted in Fig. 2 some observed radiative fluxes. The external source of the differential heating is the incoming solar insolation (line 1), a function only of the orbital parameters. With increasing albedo at high latitudes due partly to the low

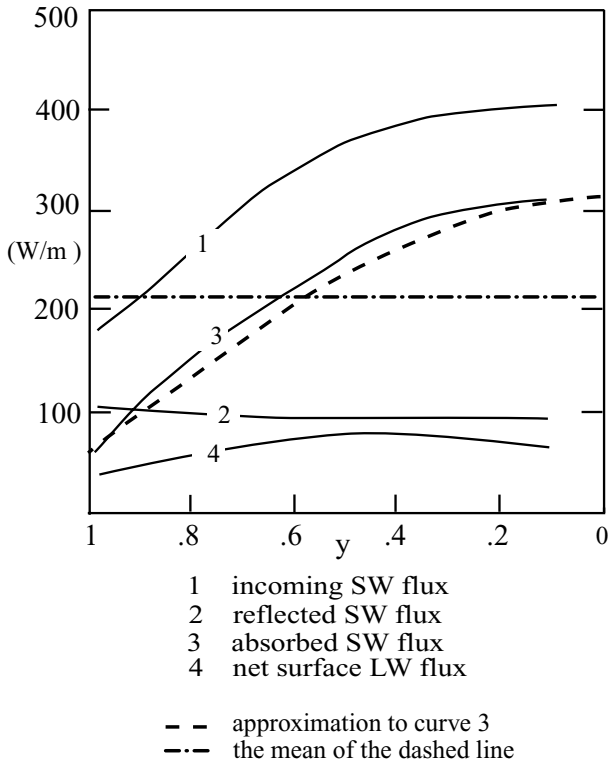

Fig. 2. Latitudinal distribution of the observed radiative fluxes. All the solid curves are taken from Figs. 6.13 and 14 of Peixoto and Oort (1992), except curve 4, which is taken from Fig. 6.25 of Liou (1992). The dash-dotted line is the mean of curve 3, and the dashed line is the approximation of curve 3 (by a quarter cycle of the cosine function) after the mean is removed.

clouds, the absorbed SW flux (line 3) turns out to be roughly a constant offset (line 2) from the solar insolation. After removing the global mean (dash-dotted line), the absorbed SW flux thus can be approximated by a quarter-cycle cosine function (dashed line) – the external forcing of the model.

Heated differentially by the absorbed solar flux, the ocean is preferentially warmed in lower latitudes, whose equator-to-pole temperature range, however, is seen later (Section 4.4) to be small compared with its absolute temperature. Combined with the small air–sea temperature difference (see Ou01) and rapidly increasing downward LW flux over the warmer water (Hartmann and Michelsen, 1993), one expects the net LW flux exiting the ocean to have a small range, as indeed observed (line 4). With the observed range about an order of magnitude smaller than that of the absorbed solar flux, it is neglected in comparison, so the only other source of differential heating of the ocean is the convective flux, which is seen later (Section 4.4) to be comparable in magnitude to the solar heating (the observed range of the convective flux is about 100 W m^{-2}, see e.g. Fig. 6.25c of Liou, 1992).

We next consider the radiative heating of the atmosphere, which is seen earlier (Section 3.1) to involve only the LW flux in the absorption band. Across its lower boundary, the net of this flux is small due to the small air–sea temperature difference, and so should be its range (this net differs from line 4 of Fig. 2, which includes the radiation in the spectral window). As a partial support, radiative-transfer calculations (Hartmann and Michelsen (1993), their Fig. 1) show this range to be in the low tens of W m^{-2} over the nominal range of the surface temperature, which is deemed small compared with that of the convective flux (see above). Across the tropopause, with the constant emission temperature of the OLR in the absorption band, there is differential heating only if this flux is partially redirected downward by high clouds, the local fraction of which depends on the tropopause temperature. How the latter is coupled to the surface temperature is unknown and likely would involve dynamical consideration outside the scope of the present model, so, for simplicity, the effect of this coupling on the entropy flux out of the atmosphere is neglected.

Based on the above discussion, we thus have a simplified heating scheme that drives the meridional thermal structure: The system is heated differentially by the solar flux absorbed by the ocean, which then heats the atmosphere differentially by the convective flux of sensible and latent heat. It is seen later that the differential thermal field is strongly constrained by intrinsic water properties, which partially justifies this extremely crude heating scheme.

3.4. Deviation fields

As the object of the model is to determine the deviation from the (known) global-mean temperature, one needs only to maximize the entropy fluxes that are affected by the deviation field, which moreover are seen above to involve only fluxes at the ocean surface. Let the respective fields for the ocean and atmosphere be decomposed into their global mean (overhats) and deviation (primes),

$$F = \bar{F} + F', \tag{3.5}$$

$$T = \bar{T} + T', \tag{3.6}$$

one has then

$$\int_0^1 F' dy = \int_0^1 T' dy = 0. \tag{3.7}$$

where the latitudinal coordinate is defined as

$$y = \sin(\theta), \tag{3.8}$$

with θ being the latitude, so an equal interval in y contains the same surface area. As alluded to earlier (Section 3.3), deviation in temperature is small compared with its global mean

$$T' \ll \bar{T}, \tag{3.9}$$

so the perturbation entropy flux in (3.4) that needs to be maximized is

$$\sigma' = \bar{T}^{-2} \int_0^1 F' T' dy, \tag{3.10}$$

in which the sign convention has been changed so the heat flux entering a fluid medium is taken to be positive.

The convective fluxes of sensible and latent heat can be combined to yield

$$F'_C = \alpha(T'_{\rm o} - T'_{\rm a}), \tag{3.11}$$

where the heat exchange coefficient α is given by

$$\alpha \equiv \rho_{\rm a} C_{\rm p,a} C_D |u'| (1 + {\rm Bo}^{-1}), \tag{3.12}$$

with ρ_a being the density of the surface air,[3] $C_{p,a}$, its specific heat at constant pressure, C_D, the drag coefficient, $|u'|$, the amplitude of the turbulent wind, and Bo, the Bowen ratio. Both turbulent wind and Bowen ratio vary spatially, but they compensate somewhat since the turbulent wind is typically weaker over the tropical oceans where the Bowen ratio is smaller. As a minimal model, there is no justification for including such variation in the heat exchange coefficient, which is thus taken to be a constant – hence given by its (known) global-mean value. Moreover, it is seen later that this value enters the model only through setting the differential temperature scale, so its effect on the thermal field can be easily discerned.

For convenience, the model derivation will be carried out in non-dimensional forms. Specifically, we scale all differential heat fluxes by the range of the absorbed solar flux ΔF_r and all temperature deviations by $\alpha^{-1}\ \Delta F_r$. Dropping all primes

[3]Given the small range in the surface air temperature (3.9) and the observed surface pressure, this density is taken to be constant, hence known from the global-mean model.

from this point on, with the understanding that all variables are non-dimensionalized deviations from their global means, the absorbed solar flux (the dashed line in Fig. 2) is then

$$F_r = \cos(\pi y/2) - 2/\pi, \tag{3.13}$$

the only external differential heating of the system, and the convective flux (3.11) becomes

$$F_c = T_o - T_a, \tag{3.14}$$

the only differential heat exchange between the ocean and atmosphere. With both fluid media reduced two thermal masses, the main task is simply to determine their temperature and their surface boundary by maximizing the boundary entropy flux (3.10) applied to both media, which is now non-dimensionalized to (dropping the prime)

$$\sigma = \int_0^1 FT dy. \tag{3.15}$$

In conjunction with the thermal field, the heat transport partition between the ocean and atmosphere are to be determined. With the above scaling, the total heat transport is

$$F_t = \int_0^y F_r dy = \frac{2}{\pi}\left(\sin\frac{\pi y}{2} - y\right), \tag{3.16}$$

which consists of an atmospheric component of

$$F_a = \int_0^y F_c dy, \tag{3.17}$$

and an oceanic component of

$$F_o = F_t - F_a. \tag{3.18}$$

4. Model field

4.1. Unconstrained solution

In adherence to our minimalistic, bottom-up approach, we first consider the MEP solution when no other physical constraints are imposed, which is referred hence as the "unconstrained" solution. Given the much shorter timescale of the atmosphere, the surface air temperature is first determined via the atmospheric MEP – given any surface ocean temperature, the latter is then constrained by the oceanic MEP. Applying (3.15) to the atmosphere and using (3.14), the atmosphere entropy flux is

$$\sigma_a = \int_0^1 F_c T_a dy = \int_0^1 (T_o - T_a) T_a dy. \tag{4.1}$$

which can be maximized against T_a to yield

$$T_a = \frac{1}{2} T_o. \tag{4.2}$$

for all y, or surface air temperature is simply half its oceanic counterpart (remember that we are referring to deviation from the global mean). More generally, so long as the ocean temperature is the only "external" variable that enters (4.1), algebraic symmetry demands a local linkage. With the ocean surface reduced to two thermal bands, so is the surface air, with their boundaries aligned at the ocean surface, as alluded to in Section 2.

To understand the solution (4.2), one notes that the entropy flux (4.1) involves the product of differential heating and temperature (the two terms in the integrand, respectively), with the former coupled to the latter. To assure a positive entropy production, the temperature range of the surface air must be smaller than that of the ocean. But as the former departs increasingly from the latter, the entropy flux first increases due to enhanced differential heating, then decreases as the differential air temperature approaches zero, one thus understands why the entropy flux peaks at some intermediate temperature-range, as reflected in (4.2).

Having applied MEP to the atmosphere, we next consider the entropy flux for the ocean. Let the temperature of the warm and cold masses be denoted by subscripts 1 and 2, the surface frontal latitude by y_1 (see Fig. 1), and the heat transport at y_1 by the

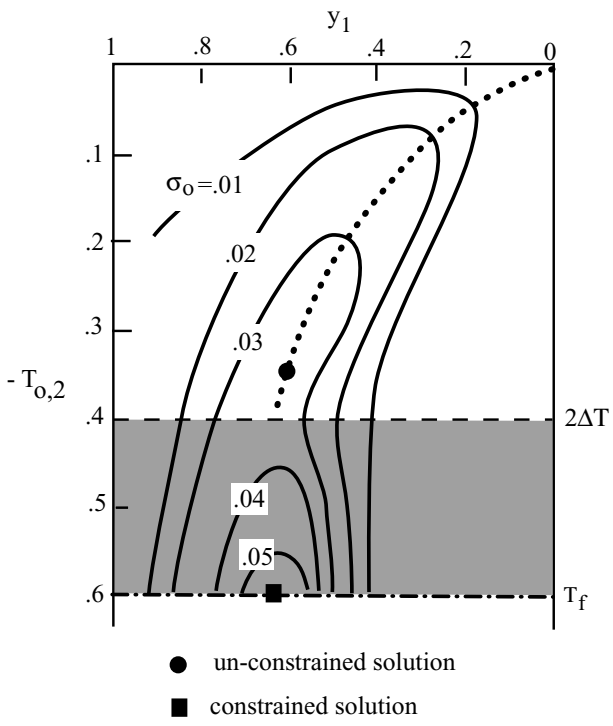

Fig. 3. The value of the ocean entropy flux as a function of the cold water temperature $T_{o,2}$ and the frontal position y_1. The dashed line marks the boundary between the unconstrained and constrained regions. The dotted line corresponds to (4.5), along which lies the unconstrained solution (4.6) marked by the solid circle. The dash-dotted line indicates the freezing point, on which lies the constrained solution (4.14) marked by the solid square.

subscript 1, respectively, the ocean entropy flux (from (3.15)) is

$$\sigma_o = \int_0^1 [F_r - (T_0 - T_a)]T_o dy$$
$$= -\frac{1}{y_1} T_{o,2}[F_{t,1} + (1 - y_1)(T_{0,2} - T_{a,2})]. \quad (4.3)$$

In arriving at (4.3), the global constraints (3.7) have been used, and the reason that (4.3) is expressed in cold temperatures will become clear later. It is noted that with the two-layer approximation, (4.3) is simply the internal entropy production (3.3) at the layer boundary as the heat flux (the bracketed term) crosses the temperature jump (the rest). Substituting (4.2) into (4.3), and maximizing the latter against $T_{o,2}$ yield

$$T_{o,2} = -\frac{1}{1 - y_1} F_{t,1}, \quad (4.4)$$

and further maximization against y_1 leads to

$$2y_1(1 - y_1)F_{r,1} - (1 - 2y_1)F_{t,1} = 0. \quad (4.5)$$

This algebraic equation can be solved numerically to yield y_1. In Fig. 3, where the ocean entropy flux is plotted against $T_{o,2}$ and y_1 (the clear area), (4.4) is indicated by the dotted line and the solution to (4.5) by the solid circle.

The thermal properties for this unconstrained solution are shown in Fig. 4a, together with the poleward heat transports calculated from (3.16)–(3.18). The atmospheric heat transport is linear in y within thermal bands since the convective heat flux is uniform within such bands, and the dimensional temperatures are based on parameter values given in the next subsection. It is seen that the temperature range of the surface air is half that of the surface ocean (4.2), the front is located at mid-latitudes, and the poleward heat transport at the front is equally partitioned between the two fluid media. This last feature can be seen from (3.17), using the constraints (3.7), (4.2) and (4.4),

$$F_{a,1} = y_1(T_{o,1} - T_{a,1})$$
$$= -(1 - y_1) \cdot (T_{o,2} - T_{a,2})$$
$$= -\frac{1}{2}(1 - y_1)T_{0,2},$$
$$= \frac{1}{2} F_{t,1}, \quad (4.6)$$

which is thus a direct consequence of MEP applied to both ocean and atmosphere. Needless to say, the solution is inadequate when compared with the present observations: the cold masses are too warm, the equator-to-pole temperature range too small, and

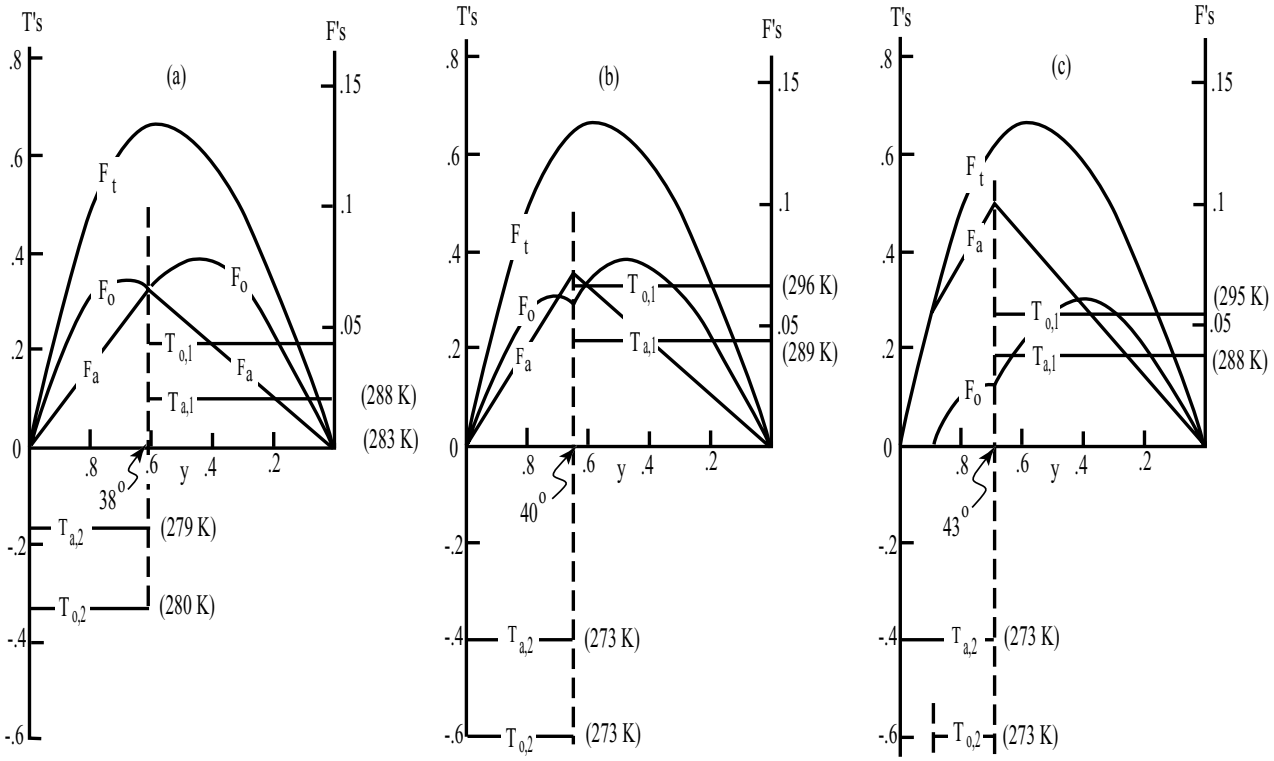

Fig. 4. (a) Thermal properties of the unconstrained solution (the solid circle in Fig. 3) plotted against sine of the latitude. The symbols T are for the surface temperatures (deviations from the global means) and F for the poleward heat transports, all non-dimensionalized. Subscripts t, o, and a are for "total," "ocean," and "atmosphere," and 1 and 2 for the warm and cold masses, respectively. The absolute temperature is based on estimates given in Section 4.2; (b) same as (a) but for the constrained solution (the solid square in Fig. 3); (c) same as (b) but includes a polar continent that extends to about 70 latitudinal degrees.

the observed heat transport is far from equally partitioned. So what is the missing physics? One clue lies in the premise of a globally convective troposphere, which was invoked to argue for its reduction to two thermal masses, and not yet explicitly incorporated in the derivation of the solution.

4.2. Constrained solution

With the surface temperature already reduced to two uniform bands, a globally convective troposphere implies that the surface air may not be warmer than the underlying ocean in either band. But given that the surface air has a smaller temperature range than the surface ocean (Section 4.1), the above condition imposes a constraint only on the cold band – since the condition is then automatically satisfied for the warm band. Now, recall that the global-mean temperatures of the surface ocean and air have been removed, and let $\Delta\bar{T}$ denote their non-dimensionalized difference, the above constraint states then

$$T_{\mathrm{a},2} - T_{\mathrm{o},2} \leq \Delta\bar{T}. \tag{4.7}$$

Substituting (4.2) into (4.7), one sees that the unconstrained solution is valid if and only if

$$|T_{\mathrm{o},2}| \leq 2\Delta\bar{T}. \tag{4.8}$$

An example of the rhs is indicated in Fig. 3 by the dashed line. If this line lies above the solid dot, then (4.8) is violated, and the unconstrained solution is untenable. But as we shall see next, regardless whether the unconstrained solution is allowed, there is *always* a MEP solution when the bound (4.8) is exceeded.

In this latter parameter range (the shaded area in Fig. 3), MEP of the atmosphere implies that the equality in (4.8) holds since (4.1) is still in its upswing toward its maximum at (4.2) (see the discussion following (4.2)). Substituting this equality in (4.8) into (4.3), the latter becomes

$$\sigma_{\mathrm{o}} = -\frac{1}{y_1} T_{\mathrm{o},2}[F_{\mathrm{t},1} - (1 - y_1)\Delta\bar{T}], \tag{4.9}$$

whose contours are plotted in the shaded area. It is seen that (4.9) increases monotonically with decreasing $T_{o,2}$, the latter, however, is bounded by the freezing point

$$|T_{\mathrm{o},2}| \leq T_{\mathrm{f}}, \tag{4.10}$$

as indicated by the dash-dotted line. Along this line, (4.9) can be maximized with respect to y_1 to yield

$$y_1 F_{\mathrm{r},1} - F_{\mathrm{t},1} + \Delta\bar{T} = 0, \tag{4.11}$$

which determines y_1, as marked by the solid square. This solution is referred as the "constrained" solution since it invokes explicitly the assumption of a globally convective atmosphere (4.7) and the natural bound on the water temperature (4.10).

In the above derivation of the constrained solution, we have assumed that the ocean remains ice-free – even though the cold water is at the freezing point. This is because the presence of sea ice would cut down the ocean cooling and reduce the ocean heat transport – in violation of MEP. It is trivial to include an unknown sea ice cover in the ocean entropy flux and see that it shrinks to zero when the latter is maximized. This deduction may possibly explain the lack of perennial sea ice around the Antarctica, in sharp contrast to the semi-enclosed Arctic Ocean.

To obtain the numerical markings shown in Fig. 3, we need to assign values to external parameters and relevant global-mean fields. So long as the latter have been determined in Ou01 to assure the physical closure, one may simply use observed values as input to the present calculations since testing of global-mean fields is not of the present concern. As such, we set $|u'| = 5$ m s^{-1} and $\mathrm{Bo}^{-1} = 1.5$ to arrive at $\alpha \approx 12.5$ W m^{-2} °K^{-1}; and with $\Delta F_r = 300$ W m^{-2}, the scale for the temperature range is then 25 °K. Using the mean ocean-air temperature difference of 5 °K and a global-mean ocean surface temperature of 288 °K, we obtain additionally $\Delta\bar{T} = 0.2$ and $T_f = 0.6$, as indicated in the figure. For the particular example shown in Fig. 3, although the unconstrained solution is allowed, the constrained solution nonetheless has a higher entropy production rate, hence should be favored in accordance with MEP.

The thermal properties for this constrained solution are shown in Fig. 4b, with the absolute temperature indicated. When compared with the unconstrained solution (Fig. 4a), the temperature range of both surface air and ocean are much greater as the cold masses are cooled to the freezing point (remember that the solution is for deviation from the global means, so the two cold bands are not aligned). And given the smallness of $\Delta\bar{T}$ that sets the temperature difference of the two cold bands, the two temperature ranges are also more comparable. These changes represent a significant improvement over the unconstrained solution when compared with the earth's climate. Moreover, since the model has so far considered a global ocean, one expects the solution to be more applicable to, say, mid-Cretaceous, when effects of polar continents are smaller, as seems to be the case (see Crowley and North, 1991, their Fig. 8.2).

Although equal partition of the heat transport at the frontal latitude no longer holds exactly for the constrained solution, the two heat transports remain comparable – a fortuitous outcome due to the selection of the $\Delta\bar{T}$ value (that is, it is close to the temperature difference between the two cold bands in the unconstrained solution). There is no proxy data on the heat transport in the geological past, but such equal partition certainly deviates far from that observed presently, which is dominated by the atmosphere beyond the tropics (Trenberth and Caron, 2001). It should be mentioned that the oceanic share of the heat transport has been revised downward significantly in recent years. Since the value of $\Delta\bar{T}$ is representative of the present climate, it cannot be tuned to remove this substantial discrepancy and other physical consideration maybe needed.

4.3. Polar continents

One plausible remedy is the presence of polar continents, which would block the ocean heat transport. But does it have a global impact as needed? To address this question, it suffices to consider a small continent so as not to upset the global balances.

Let the edge of the polar continents be denoted by y_i (assuming hemispheric symmetry for simplicity), then the total heat transport there $F_{t,i}$ is carried solely by the atmosphere, or

$$F_{\mathrm{t,i}} = y_1(T_{\mathrm{o},1} - T_{\mathrm{a},1}) + (y_{\mathrm{i}} - y_1)(T_{\mathrm{o},2} - T_{\mathrm{a},2}). \tag{4.12}$$

It is easily seen that the ocean entropy flux (4.12) is modified to

$$\sigma_o = \frac{1}{y_1} T_f [F_{t,1} - F_{t,i} - (y_i - y_1)\Delta\bar{T}] \tag{4.13}$$

so that, instead of (4.14), the frontal boundary is governed by

$$y_1 F_{r,1} - (F_{\mathrm{t},1} - F_{\mathrm{t,i}} - y_{\mathrm{i}}\Delta\bar{T}) = 0. \tag{4.14}$$

As a check, if one sets $y_i = 1$ and $F_{t,i} = 0$, these equations reduce to their previous forms.

Using the same parameter values cited above and $y_i = 0.9$ (polar continents extending to about 70 latitudinal degrees), the thermal properties of the solution are plotted in Fig. 4c. When compared with Fig. 4b, there is sharp reduction of the ocean heat transport beyond the tropics, which is thus more in line with the present-day observation. But despite such large change in the heat transport, the temperature of the fluid masses and the frontal boundary remain virtually unchanged. It should be mentioned that although the cold air temperature remains at the freezing point at the sea level given the smallness of the continent, the elevation of the latter could yield a much colder surface air on account of the lapse rate.

Since both the thermal field and the heat transport partition now seem reasonable given the limitation of an extreme crude model, we suspect that the model has captured the minimal physics for the observed field. Based on the formal derivation of the model climate, we thus offer the following synthesis of its underlying physics.

4.4. Synthesis

We begin with the ocean, which has been divided into warm and cold masses defined by forced and free convection. With such reduction, the entropy is produced internally only at the layer boundary where heat is transported across a temperature jump, and both tend to maximum according to MEP. Maximizing the heat transport implies firstly that the ocean be free of ice (since ice would cut down the surface cooling and hence the poleward heat transport) and secondly that the front be located at mid-latitudes (since the heat transport is zero at the equator and pole). To maximize the temperature jump on the other hand propels the cold-water temperature to its lower natural bound – the freezing point. Combined with a mid-latitude front and hence a temperature range roughly centered about the global mean temperature, the warm water temperature thus is known. Incidentally, given the small deviation of the freezing point from the global-mean temperature, the range in the surface temperature is an order of magnitude smaller that its absolute value, which provides a posteriori justification of (3.9) for the surface ocean.

For the atmosphere, being dominated by differential heating from the ocean surface, the reduction of the latter to two thermal bands implies the same for the surface air on account of MEP, which leads via free convection to tropical and polar air masses homogenized in equivalent potential temperature. To maximize the atmospheric heat transport, its temperature range must decrease sufficiently from that of the ocean, or that the polar air be sufficiently warm. But the latter may not be warmer than the underlying ocean surface for a convective troposphere, which thus attains the freezing temperature as well. Again, the temperature range should roughly center at its global mean, thus specifying the tropical air temperature. With the temperature range of the surface air smaller than that of the surface ocean, it again supports the assumption (3.9) for the surface air.

Now about the poleward heat transport, the total is set by the differential heating due to the absorbed solar flux, which is similar to the incoming solar flux (Fig. 2), hence known. For the atmospheric portion, it is caused by the differential heating due to convective flux from below, the range of which is commensurate with (within about a factor of two) its global-mean since such flux vanishes over the cold band. It is thus by the fortuity of the strength of the global-mean convective flux that, in an aquatic earth, the atmospheric heat transport should take up about half the total, which is thus approximately equi-partitioned between the two fluid media. The presence of polar continents would locally block the ocean heat transport, but because of the rigidity of the thermal field as synthesized above, such blockage would have extended spatial impact, leading to wholesale reduction of the ocean heat transport outside the tropics.

5. Summary

The object of the study is to derive the meridional thermal field given the global-mean fields, the latter assumed determined from global-mean models. The essential closure assumption is MEP, viewed as a selection rule for the turbulent fluids. As such, MEP should apply individually to the ocean and atmosphere, and radiative fluxes affect the internal entropy production only when they interact with the fluids.

Distinguishing forced and free convective regimes of the ocean, and applying MEP to the atmosphere, both fluids are reduced two thermal masses with their boundaries aligned at the ocean surface – consistent with a minimal description of the observed climate. On account of different radiative properties of low and high clouds, they are expelled by MEP to polar and equatorial regions, respectively – a tendency discernible from observation, which thus can be explained. Given the global cloud

covers, the cloud distribution and its effect on radiative fluxes are thus known, which aids a simplified heating scheme: the system is heated differentially by the solar flux absorbed by the ocean, which then heats the atmosphere differentially through the convective flux of sensible and latent heat.

With above simplifications, a straightforward application of MEP led to an "unconstrained" solution, which, however, is characterized by too small a temperature range for both fluids and an equal partition of the heat transport that deviates far from the present observation. Incorporating bounds on a convective troposphere and water temperature, an additional "constrained" solution is found, which has reasonable temperature range as the cold fluid masses are cooled to the freezing point, but the discrepancy in the heat transport remains. This last shortfall can be removed by a small polar continent, which drastically reduces the ocean heat transport beyond the tropics, but leaves the thermal field largely unchanged.

With the derived field now seems reasonable – given the limitation of an extremely crude model, it is suggested that the model has captured sufficient physics for a minimal account of the observed field.

6. Discussion

Since the global mean fields are determined by applying MEP to a one-dimensional vertical model (Ou01), the tacit assumption is that this maximum is not altered by the inclusion of the meridional dimension (see also Ozawa and Ohmura, 1997). This obviously is the case if there is no differential heating to induce meridional structure, but since the meridional temperature deviates only slightly from the global mean (less than 10%), one expects the assumption to approximately hold. Moreover, MEP in the vertical model is due to convection, somewhat independent of the horizontal motion that yields MEP in a meridional field, further justifying their separate applications. This is in fact reflected in Paltridge's (1975) closure, an issue also discussed by Pujol and Llebot (2000).

The model differs from Paltridge (1975) in many important ways. For example, the additional physical consideration (of distinct convective regimes) leads paradoxically to a simpler system consisting of few thermal masses, an observed feature that can now be explained. By applying MEP to the ocean and atmosphere individually, there is no need to assign transport partition between the two in the model, which should be an internal property of the system. The model distinguishes the ocean and air temperature to facilitate convective heat exchange. Above all, with its minimal construct, the model contains no tunable parameters and can be more critically tested.

In Ou01, we have seen that the global-mean surface temperature is narrowly constrained by intrinsic water properties to lie slightly (in the absolute scale) above its triple point: the two bounds being related to the rapid increase in – successively – the greenhouse warming and evaporate cooling as the temperature rises above the triple point. In the present derivation, we see additionally that cold fluid masses would attain the freezing point on account of MEP that maximizes the thermal contrast. The study thus reinforces the controlling role of the triple point on the surface temperature (Webster, 1994), stabilizing it against changing external conditions. Such internal control in fact justifies the extreme simplification of the model, and it is made possible by the turbulent nature of the ocean and atmosphere that necessitates a selection rule based on extremization.

This stability of the thermal field, however, does not carry over to the heat transport – perhaps a fortunate happenstance since only temperature has sensory significance. While the total poleward heat transport is linked to the differential solar heating, it can be wholesale redistributed between the two fluids by a small polar continent – due in fact to the rigidity of the thermal field. This subsidiary role played by the heat transport on the thermal field is somewhat counter-intuitive, but nonetheless conceivable since, for the long timescale that defines the climatic state, the temperature can adjust to whatever is required by the global balance regardless the heat transport. The relatively weak ocean heat transport in the present climate does not, however, lessen its importance on the air temperature since the atmosphere – being differentially heated by the ocean – can be warm only over warm water, as reflected in the alignment of the two fronts.

The breaking of the direct linkage between heat transport and temperature gradient underscores the futility of eddy diffusivity, a concept rendered unnecessary in the present formalism. In fact, the emergence of internal boundaries suggests that the eddy diffusivity, if it were to be used, is highly heterogeneous – being strongly curtailed at these boundaries. Depriving the system of such degrees of freedom by some energy-balance models could be the root cause of undue sensitivity of their climate, including a run-away to ice-covered earth when the sun is only slightly dimmed (Budyko, 1969). The use of an extremization principle, on the other hand, invariably leads to a more stable climate, consistent with previous findings (Gerard et al., 1990; Lorenz et al., 2001), and the application of MEP in particular yields an ice-free ocean (Section 4.2) that deactivates the ice-albedo feedback. It should be stressed that the model considers a global ocean punctuated at most by a small polar continent, so it does not preclude the possibility of a snowball earth if there are extensive continents (Hartland and Rudwick, 1964).

Since the model contains no explicit dynamics and yet produces a reasonable climate, it reinforces the premise of energy-balance models that the surface temperature is largely controlled by thermodynamics. On the other hand, since thermal boundaries mark strong flows in a rotating system (the thermal wind), the general circulation of the ocean and atmosphere can be properly addressed only within such thermal constraints. As the mixing of thermal property within fluid masses has its dynamical counterpart in the potential vorticity (Rhines and Young, 1982), this feature may be explored for its implications on the general circulation, a topic to be discussed in future papers.

7. Acknowledgments

I want to thank my colleagues at Lamont for spirited discussions during the long years when the theory is gradually taking shape, and Axel Kleidon and anonymous reviewers for comments on the earlier drafts, which have significantly improved the paper. I also want to thank Dr. Jay Fein of NSF for his foresight in supporting the work through grant ATM-0334731. The paper has the L-DEO contribution number 6832.

References

Budyko, M. I. 1969. The effect of solar radiation variations on the climate of the Earth. *Tellus* **21**, 611–619.

Crowley, T. J. and North, G. R. 1991. *Paleoclimatology*. Oxford University Press, New York, 339.

De Groot, S. R. and Mazur, P. 1984. *Non-Equilibrium Thermodynamics*. Dover Publications, Inc., New York, 510.

Dewar, R. 2003. Information theory explanation of the fluctuation theorem, maximum entropy production and self-organized criticality in non-equilibrium stationary states. *J. Phys. A Math. Gen.* **36**, 631–641.

Essex, C. 1984. Radiation and the irreversible thermodynamics of climate. *J. Atmos. Sci.* **41**, 1985–1991.

Gerard, J., Delcourt, D. and Francois, L. M. 1990. The maximum entropy production principle in climate models: application to the faint young sun paradox. *Q. J. R. Meteorol. Soc.* **116**, 1123–1132.

Hartland, W. B. and Rudwick, M. J. S. 1964. The great infra-Cambrian glaciation. *Sci. Am.* **211**, 28–36.

Hartmann, D. L. 1994. *Global Physical Climatology*. Academic Press, Inc., San Diego, 411.

Hartmann, D. L. and Michelsen, M. L. 1993. Large-scale effects on the regulation of tropical sea surface temperature. *J. Clim.* **6**, 2049–2062.

Hill, A. 1990. Entropy production as the selection rule between different growth morphologies. *Nature* **348**, 426–428.

Jaynes, E. T. 1957. Information theory and statistical mechanics. *Phys. Rev.* **106**, 620–630.

Jaynes, E. T. 1980. The minimum entropy production principle. *Ann. Rev. Phys. Chem.* **31**, 579–601.

Kleidon, A. 2004. Beyond Gaia: thermodynamics of life and earth system functioning. *Clim. Change* **66**, 271–319.

Kleidon, A., Fraedrich, K., Kunz, T. and Lunkeit, F. 2003. The atmospheric circulation and states of maximum entropy production. *Geophys. Res. Lett.* **30**(23), 2223, doi: 10.1029/2003GL018363.

Liou, K. N. 1992. *Radiation and Cloud Processes in the Atmosphere. Theory, Observation, and Modeling*. Oxford University Press, New York, 487.

Lorenz, E. W. 1960. Generation of available potential energy and the intensity of the general circulation. In: *Dynamics of Climate* (ed. R. L. Pfeffer). Pergamon Press, Tarrytown, New York, 86–92.

Lorenz, R. D., Lunine, J. I., Withers, P. G. and Mckay, C. P. 2001. Titan, Mars and Earth: entropy production by latitudinal heat transport. *Geophys. Res. Lett.* **28**, 415–418.

Malkus, W. V. R. 1954. The heat transport and spectrum of thermal turbulence. *Proc. R. Soc. Lond.* **A225**, 196–212.

Malkus, W. V. R. 1956. Outline of a theory of turbulent shear flow. *J. Fluid Mech.* **1**, 521–539.

Marotzke, J. and Stone, P. H. 1995. Atmospheric transports, the thermohaline circulation, and the flux adjustments in a simple coupled model. *J. Phys. Oceanogr.* **25**, 1350–1364.

Minobe, S., Kanamoto, Y., Okada, N., Ozawa, H. and Ikeda, M. 2000. Plume structures in deep convection of rotating fluid. *Nagare* **19**, 395–396. (available at http://www.nagare.or.jp/mm/2000/minobe/index.htm.)

Neumann, G. and Pierson, W. J., Jr. 1966. *Principles of Physical Oceanography*. Prentice-Hall, Englewood Cliffs, New Jersey, 545.

O'Brien, D. M. and Stephens, G. L. 1995. Entropy and climte. II: simple models. *Q. J. R. Meteorol. Soc.* **121**, 1773–1796.

Ou, H. W. 2001. Possible bounds on the earth's surface temperature: from the perspective of a conceptual global-mean model. *J. Clim.* **14**, 2976–2988.

Ozawa, H. and Ohmura, A. 1997. Thermodynamics of a global-mean state of the atmosphere – a state of maximum entropy increase. *J. Clim.* **10**, 441–445.

Ozawa, H., Ohmura, A., Lorenz, R. D. and Pujol, T. 2003. The second law of thermodynamics and the global climate system: a review of the maximum entropy production principle. *Rev. Geophys.* **41**, 4/10182003, doi: 10.1029/2002RG000113.

Ozawa, H., Shimokawa, S. and Sakuma, H. 2001. Thermodynamics of fluid turbulence: a unified approach to the maximum transport properties. *Phys. Rev.* **E64**, 026303–1–8.

Palmen, E. and Newton, C. W. 1969. *Atmospheric Circulation Systems*. Academic Press, New York, 606.

Paltridge, G. W. 1975. Global dynamics and climate – a system of minimum entropy exchange. *Q. J. R. Meteorol. Soc.* **101**, 475–484.

Paltridge, G. W. 1978. The steady-state format of global climate. *Q. J. R. Meteorol. Soc.* **104**, 927–945.

Pauluis, O. and Held, I. M. 2002. Entropy budget of an atmosphere in radiative–convective equilibrium. Part I: maximum work and frictional dissipation. *J. Atmos. Sci.* **59**, 125–139.

Peixoto, J. P. and Oort, A. H. 1992. *Physics of Climate*. American Institute of Physics, New York, 520.

Prigogine, I. 1967. *Thermodynamics of Irreversible Processes*, 3rd Edition. John Wiley & Sons, New York, 147.

Pujol, T. and Llebot, J. E. 2000. Extremal climatic states simulated by a 2-dimensional model. Part I: sensitivity of the model and present state. *Tellus* **52A**, 422–439.

Rhines, P. B. and Young, W. R. 1982. Homogenization of potential vorticity in planetary gyres. *J. Fluid Mech.* **122**, 347–367.

Rogers, C. D. 1976. Comments on Paltridge's 'Minimum entropy exchange principle'. *Q. J. R. Meteorol. Soc.* **102**, 455–457.

Rossby, H. T. 1965. On thermal convection driven by non-uniform heating from below: an experimental study. *Deep Sea Res.* **12**, 9–16.

Sawada, Y. 1981. A thermodynamic variational principle in nonlinear non-equilibrium phenomena. *Prog. Theor. Phys.* **66**, 68–76.

Shimokawa, S. and Ozawa, H. 2002. On the thermodynamics of the oceanic general circulation: irreversible transition to a state with higher rate of entropy production. *Q. J. R. Meteorol. Soc.* **128**, 2115–2128.

Stommel, H. 1961. Thermohaline convection with two stable regimes of flow. *Tellus* **13**, 224–230.

Suzuki, M. and Sawada, Y. 1983. Relative stabilities of metastable states of convecting charge-fluid systems by computer simulation. *Phys. Rev. A* **27**, 478–489.

Swinbank, W. C. 1963. Long-wave radiation from clear skies. *Q. J. R. Meteorol. Soc.* **89**, 339–348.

Trenberth, K. and Caron, J. 2001. Estimates of meridional atmosphere and ocean heat transports. *J. Clim.* **14**, 3433–3443.

Veronis, G. 1973. Model of the world ocean circulation: I. Wind-driven, two-layer. *J. Mar. Res.* **31**, 228–288.

Webster, P. J. 1994. The role of hydrological processes in ocean-atmosphere interactions. *Rev. Geophys.* **32**, 427–476.

Ziegler, H. 1983. *An Introduction to Thermomechanics* Volume 21 of Applied mathematics and mechanics, 2nd Edition. North Holland, Amsterdam.